Available online at www.sciencedirect.com
ScienceDirect
Bioelectrochemistry 70 (2007) 104–114
Bioelectrochemistry
www.elsevier.com/locate/bioelechem

A new exposure system for the *in vitro* detection of GHz field effects on neuronal networks

Philipp Koester [a], Jan Sakowski [a], Werner Baumann [a], Hans-Walter Glock [b], Jan Gimsa [a,*]

[a] *University of Rostock, Institute of Biology, Chair of Biophysics, Gertrudenstr. 11A, D-18057 Rostock, Germany*
[b] *Faculty of Computer Science and Electric Engineering, Chair of Theoretical Electrotechnics, Albert-Einstein-Str. 2, D-18051 Rostock, Germany*

Received 15 June 2005
Available online 18 April 2006

Abstract

The possible effects of high-frequency electromagnetic fields (EMF) on biological systems are a subject of public concern and scientific discussion. It is generally accepted that the absorption of part of the field energy may cause a temperature rise in biological tissue. Nevertheless, our setup aims to detect possible athermal effects on the electric activity of neuronal *in vitro* networks. Such networks were formed by primary neurons derived from the murine frontal cortex and cultivated on micro-sensor chips. The action potentials of the neurons were detected in real time by an integrated, electrically passive microelectrode array. For EMF exposure, the chips were introduced into a rectangular wave-guide that could be operated in the propagating or standing wave modes. The drive signals were either continuous waves (1.9–2.2 GHz) or a generic mobile phone signal (UMTS-standard) of up to approximately 8 W. An on-chip sensor allowed the temperature progression to be recorded. In addition, ISFETs and Clark-like electrodes were integrated for the on-chip detection of pH and O_2, respectively.

Keywords: Multi-electrode array; Micro-sensor chip; Biochip; EMF; UMTS; Wave-guide

1. Introduction

Different ideas exist about possible targets for biological effects of electromagnetic fields (EMF). One of the favorite systems is the membrane of nerve cells, e.g., in the central nervous system. In our experiments, we expose neuronal networks to EMF and conduct direct electrophysiological measurements, i.e., detect the action potential pattern produced by the networks. Our aim is to clarify whether EMF exposure may induce athermal effects. The technique was developed as an alternative to the common patch-clamp approach.

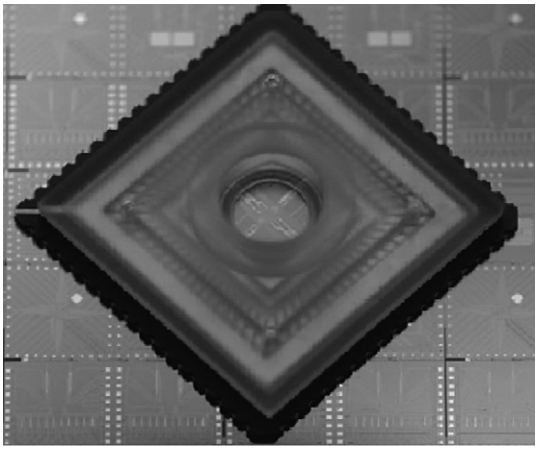

Fig. 1. Micro-sensor chip with fluid trough. The MEA is located in the center of the chip. Magnification is 2.3-fold.

Abbreviations: CMOS, complementary metal oxide semiconductor; CW, continuous wave; DMEM, Dulbecco's Modified Eagle's Medium with 4.5 g glucose/l, without Na-pyruvate, without L-glutamine; D1SGH buffer, NaCl, 135 mM; , KCl, 5 mM; , Na_2HPO_4, 0.3 mM; , KH_2PO_4, 0.2 mM; , glucose, 16.5 mM; , sucrose 22 mM; , HEPES, 9.86 mM, pH 7.35; EMF, (high-frequency) electromagnetic field; FDD, frequency division duplex; ISFETs, ion-sensitive field effect transistors; MEA, multi-electrode array; NMRI mice, outbreed white mice stem (Charles River Laboratories GmbH, Sulzfeld, Germany); SAR, specific absorption rate; UMTS, universal mobile telecommunications system

* Corresponding author. Tel.: +49 381 498 6020; fax: +49 381 498 6022.
E-mail address: jan.gimsa@uni-rostock.de (J. Gimsa).

1567-5394/$ - see front matter © 2006 Elsevier B.V. All rights reserved.
doi:10.1016/j.bioelechem.2006.03.039

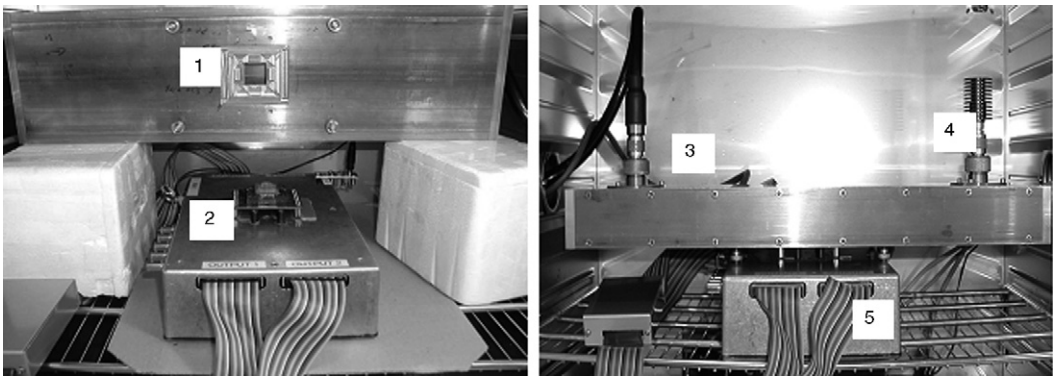

Fig. 2. Left: the wave-guide (1) is countersunk to pick up the micro-sensor chips in the socket (2). Right: view on the wave-guide with incoming signal line (3) and terminating resistor (4). The pre-amplifier is directly located under the chip socket (5). For actual experiments, the terminating resistor was connected via an extension cord and located outside the incubator to avoid an additional heat source.

Murine neurons can be grown on glass chips [3,4]. Our advanced silicon chip, developed in co-operation with Micronas-GmbH, Freiburg, Germany, combines a multi-electrode array (MEA) for the detection of neuronal activity and actual semiconductor structures allowing for the detection of different physical and metabolic parameters [1,6]. Nevertheless, neuronal adherence requires a special treatment of the silicon surface [8]. As a trade-off, additional sensors for pH or O_2 can easily be integrated on the chip.

An EMF-exposure chamber is constructed under three demands: HF tightness of the total structure, interpretation for the Universal Mobile Telecommunications System

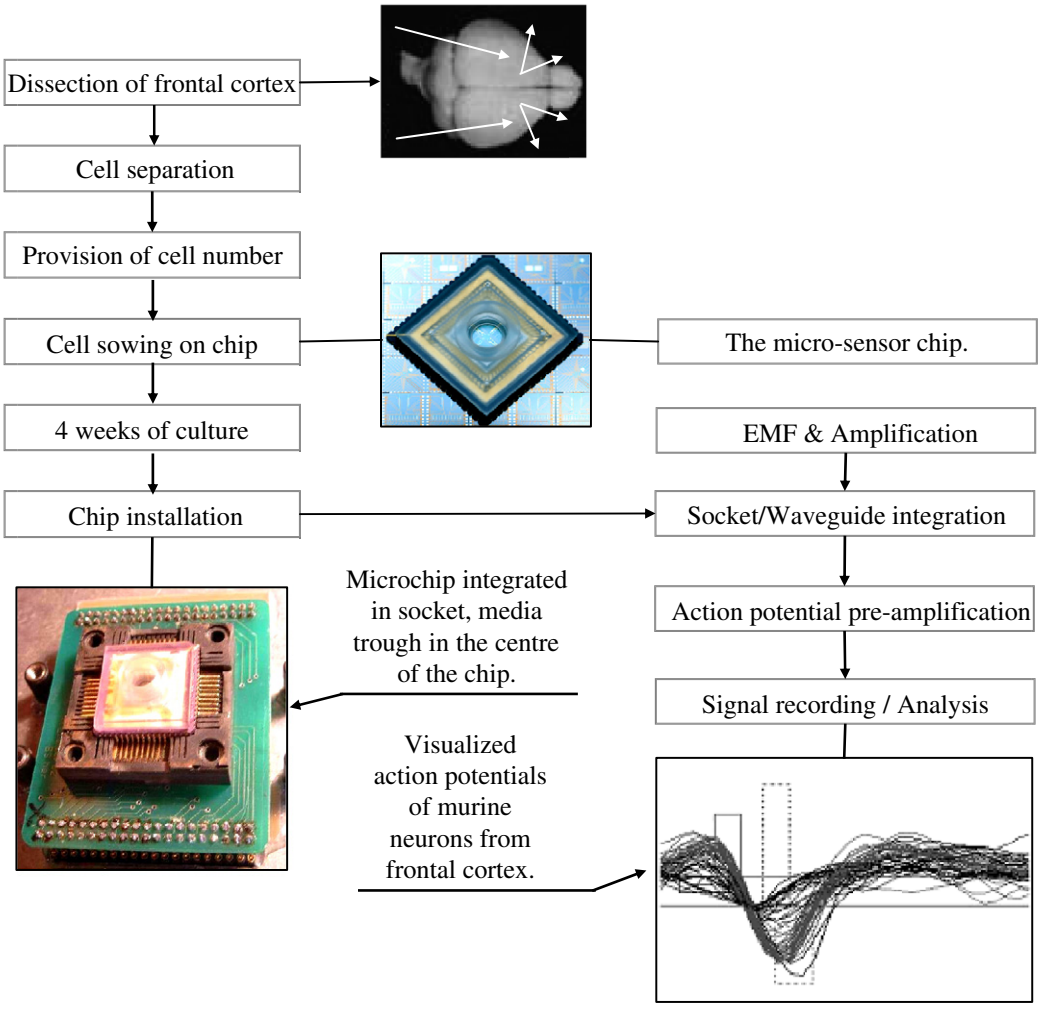

Fig. 3. Schematic representation of the experimental procedures and the setup.

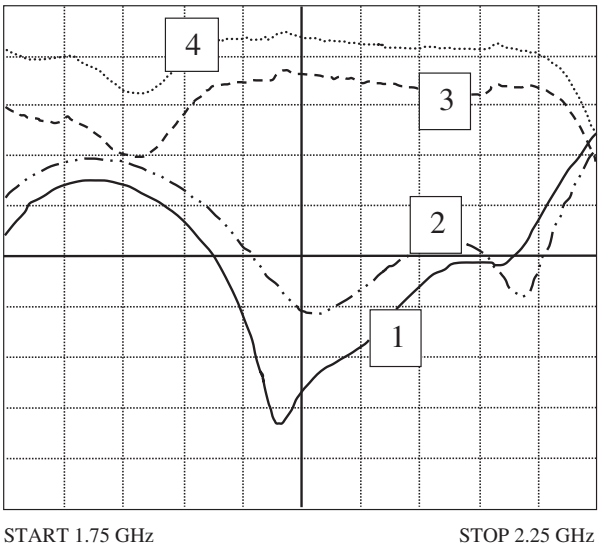

Fig. 4. Reflection (scale bars: 5 dB) and transmission (scale bars: 0.1 dB) of the wave-guide input signal in the presence and absence of the chip. Frequency range: 1.75–2.25 GHz. (1) Reflection with closed chip recess; (2) reflection with chip; (3) transmission with chip; (4) transmission with closed chip recess.

(UMTS) frequency range and access of the micro-sensor chip into the wave-guide without short circuit or EMF exposure of the measuring contacts. This wave-guide is made of brass and is specially designed for the desired wavelength and the micro-sensor chip. The wave-guide [5] was modified for our experiments. The chip fits into a recess of the wave-guide to ensure that only the chip surface, the medium trough and the neuronal cells rise into the wave-guide.

Our exposure system opens a new way for the measurement of possible functional field-induced membrane effects by continuous-wave EMF (CW EMF) and third-generation mobile communication signals (UMTS) on interneuronal communication.

2. Setting up networks from primary neurons

Primary neuronal and glial cells were isolated from the frontal cortex of embryonic (E15–E17) NMRI mice (Charles River Laboratories GmbH., Sulzfeld, Germany). The cortex tissue preparation was conducted under sterile conditions in D1SGH buffer [2]. The tissue fragments were chopped before segregation in 3 ml of a papain solution (10 U/ml, Roche Diagnostics GmbH, Mannheim, Germany) in deionized water supplemented with 50 µl of dissolved desoxyribonuclease I (8000 U/ml, Roche). The obtained homogenate was then triturated in DMEM (Biochrom AG, Berlin, Germany) supplemented with 10% fetal bovine serum (PAA Laboratories

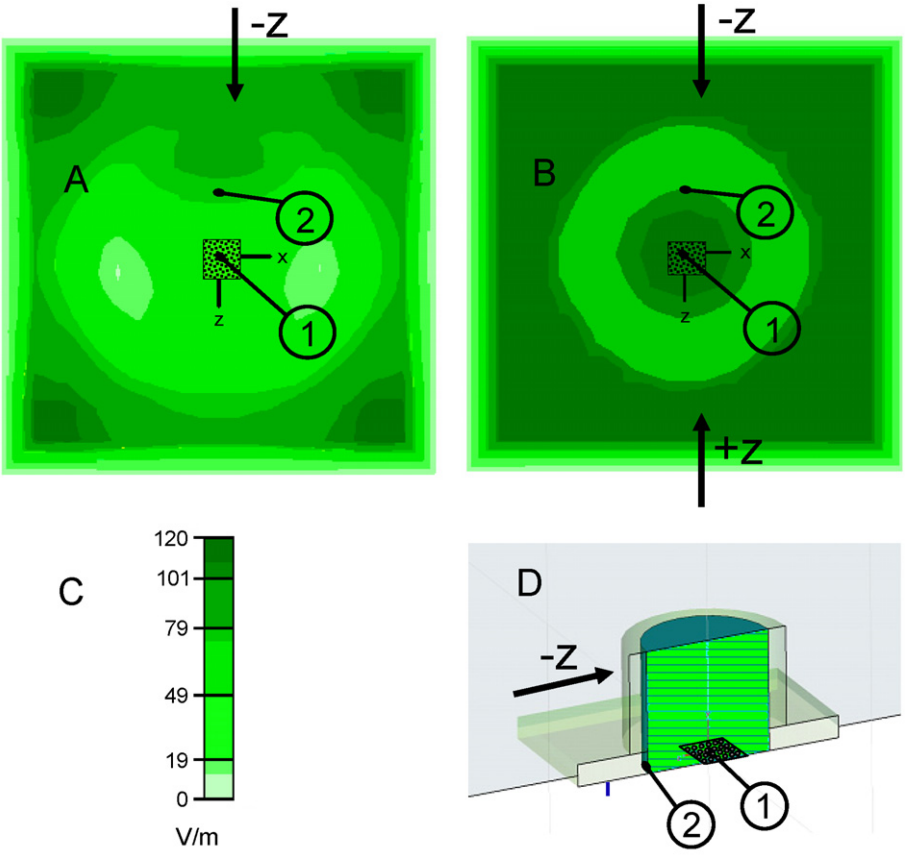

Fig. 5. Field distribution across the neuro-chip in the plane of the neuronal net location for the propagating (A) and standing wave (B) modes, calculated with CST Microwave Studio. The MEA location is marked by the dotted square in the center. At points (1) and (2) the field strengths are 58 V/m and 82 V/m (mode A) as well as 116 V/m and 93 V/m (mode B). (C) Field strength code bar. (D) Schematic view of the trough geometry. Wave propagation along the *z*-axis of the wave-guide may have two directions, + and −, respectively.

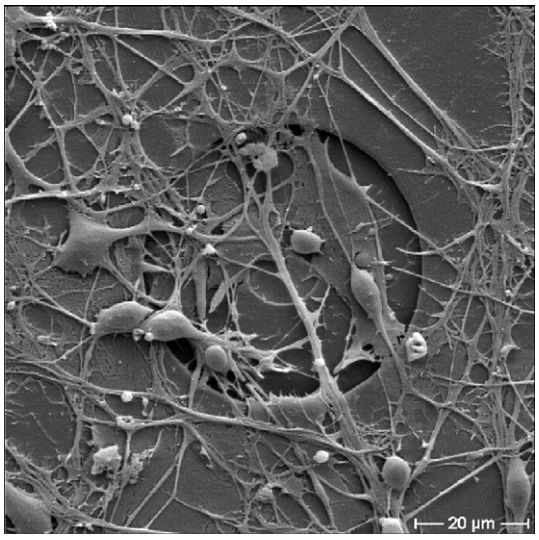

Fig. 6. REM photo of neuronal and glial cells on the micro-sensor chip. Inner electrode diameter 10 µm.

GmbH, Cölbe, Germany), 10% equine serum (Biochrom) and 1% L-glutamine (200 mM, Biochrom).

To inhibit proliferation of the glial cell population, 100 µL of a DMEM (Biochrom) solution supplemented with fluorodesoxyuridine (50 µM, Sigma-Aldrich Chemie GmbH, Taufkirchen, Germany) and uridine (126 µM, Sigma-Aldrich) was added to the on-chip cultures depending on cell concentration. To dispose metabolic waste, half of the medium of each chip culture was replaced by fresh, pre-warmed DMEM containing 10% equine serum three times a week. Cultures were maintained at 37 °C in a 10% CO_2 atmosphere for 30 days. After about 2 weeks, the cultures started to exhibit electric activity in the form of action potentials. Generally, the full activity was observed after about 4 weeks and the networks were considered mature and suitable for experiments.

3. Experimental setup

3.1. Micro-sensor chips

Our chips combine a passive MEA of 58 microelectrodes for the acquisition of action potentials and silicon CMOS technology for implementing ISFETs (ion-sensitive field effect transistors) for pH measurement as well as a temperature diode [6] The diode is located underneath the cell layer and allows for real-time temperature detection. The chips were developed by our group [1] and are fabricated by Micronas GmbH, Freiburg, Germany, (Fig. 1, Bionas GmbH, Warnemuende, Germany). A special chip socket was developed to register the electric activity of the cultivated neurons inside a wave-guide during EMF exposure.

3.2. Chip pre-treatment

The chips were cleaned with trypsin (Biochrom) and Contrad®70 (Decon Laboratories Inc., King of Prussia, PA, USA) prior to rinsing with deionized water. After that, the chips were sterilized in a Systec 2540 EL autoclave (Systec GmbH, Wettenberg, Germany). The active chip area was hydrophilized with 30 µl NaOH (0.5 M) and again rinsed with deionized water. After coating the chips with 30 µl poly-D-lysine (25 µg/ml, Biochrom) overnight, they were coated with 30 µl laminin (16 µg/ml, Roche Diagnostics) in cold DMEM for 1 h prior to cell sowing. This procedure ensured the adherence of the neurons to the micro-sensor surface.

4. Exposure setup

4.1. The wave-guide

Originally, the wave-guide was designed in the group of Prof. Hansen, Univ. of Wuppertal [5]. Its cross-sectional area is 12 cm by 3 cm at a length of 50 cm. Starting from this design, we

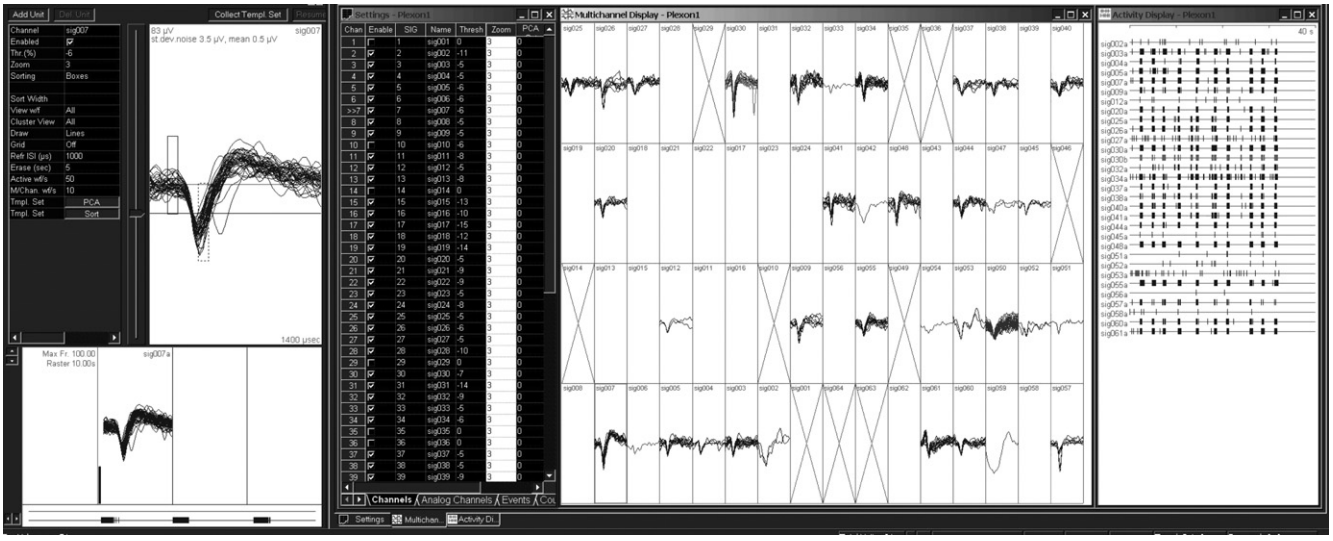

Fig. 7. Screen shot of action potentials. Left: separated single action potential. Middle: sketch of 31 active electrodes, crossed boxes show electrodes with a high noise level. Right: burst trains relative to time scale of 40 s. No EMF applied.

modified the coupling antennas slightly and adapted the countersunk recess in order to mount the chip (Fig. 2). Our design allows for establishing a fundamental wave mode at f_C=1.25 GHz and for a stable operation in the range from 1.25 f_C to 1.9 f_C, i.e., from 1.56 GHz to 2.38 GHz [7]. In this frequency range higher excitation modes are negligible since they decline sufficiently fast over the distance from the coupling antennas to the sample that is located in the center of the wave-guide. For a given input power, the width-to-height ratio of 4 deviating from the standard ratio of 2 results in a doubling of the electric power density in the sample. Fig. 2 presents a photo of the wave-guide in the cell culture incubator. The wave-guide has 2-mm drill holes for gas supply (10% CO_2 in synthetic air).

4.2. High-frequency (HF) signal sources

4.2.1. Continuous wave (CW)

To drive the wave-guide in the standing or propagating wave modes, the signal of a Marconi 2024 synthesised signal generator (Marconi Instruments/IFR, now Aeroflex; Plainfield, NY, USA) was coupled into the wave-guide via an HF amplifier (Microwave Amplifiers Ltd., Nailsea, UK) delivering approximately 8 W. Analysis showed that replacing the terminating resistor by an open coaxial cable with an appropriate length provided a maximum standing wave amplitude at the sample location as detected by a probe antenna. The cable length was experimentally determined and differed slightly from the theoretical length of a quarter of a wavelength.

4.2.2. Generic UMTS signal

Alternative to the CW exposure, a generic UMTS-signal generator (GUS 6960 S, Univ. of Wuppertal, Germany) allows for establishing the “worst case” scenario: FDD (frequency division duplex) at a simulated data rate of 960 kbit/s [9]. Because of the signal content UMTS exposure can only be simulated in the propagating wave mode.

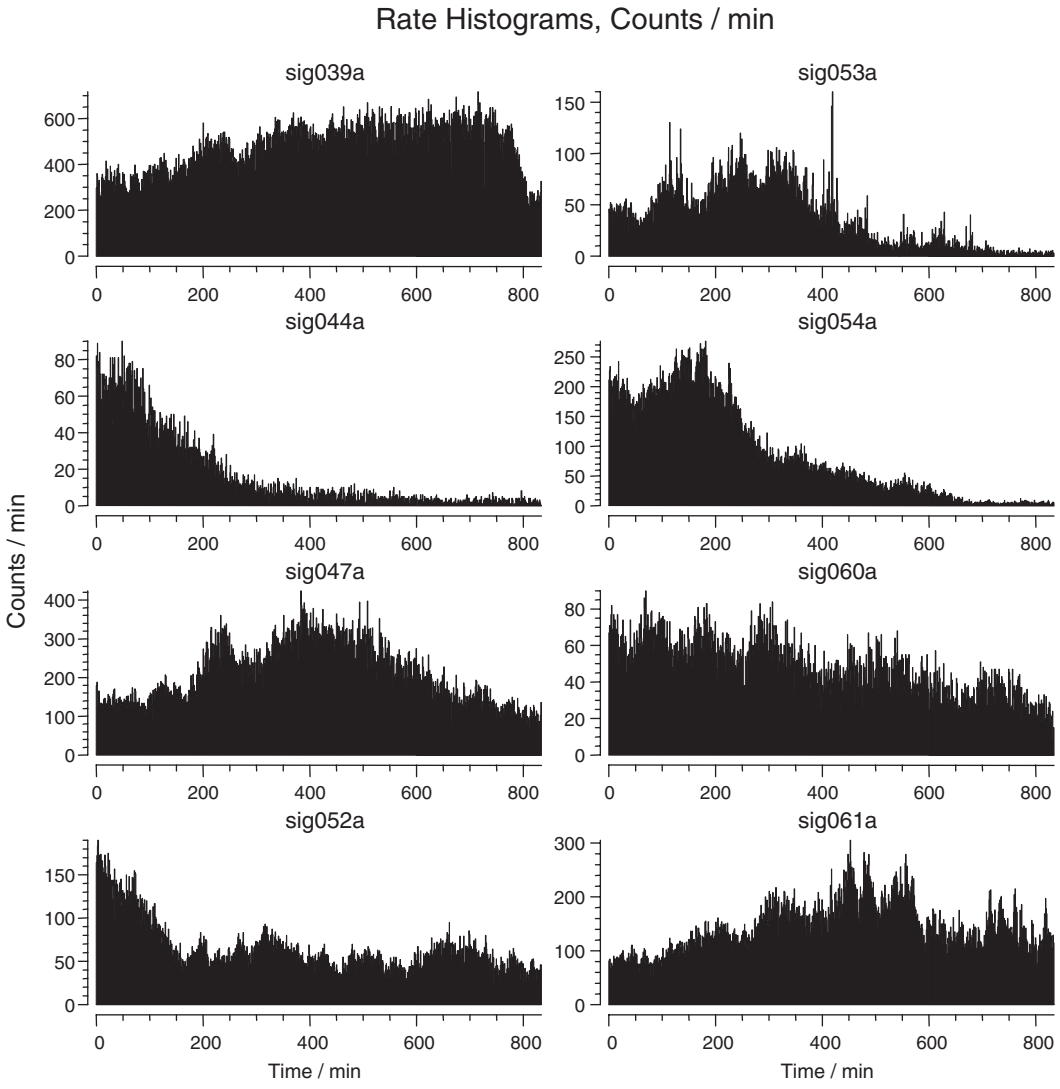

Fig. 8. Burst rates over time for control chips with no EMF applied (measurement overnight, for approximately 14 h). The neuronal activity decreased during the experiment. 8 signal traces out of 31 were selected.

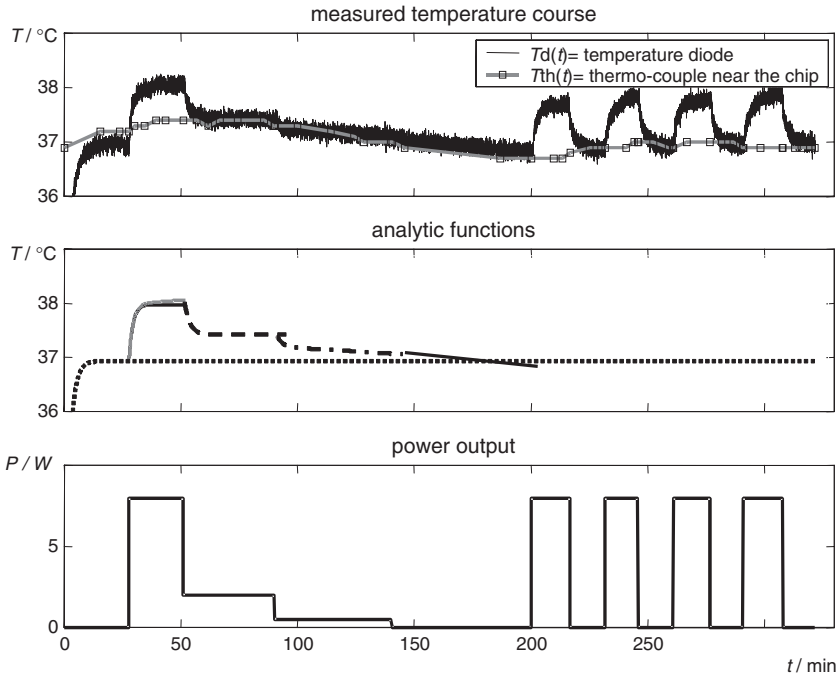

Fig. 9. Temperature patterns as functions of the applied EMF power. Top: temperatures measured by T_d (on-chip temperature diode) and T_{th} (separate sensor in the proximity of the chip). Center: fitted functions, for analytic expressions, see Table 1. Bottom: applied EMF power.

4.3. Signal acquisition

The individual action potential pattern of a neuronal network registered by the MEA generates an electronic signature for each active chip. Signature alterations can be detected depending on medium pH, temperature, EMF amplitude and exposure mode. Temperature changes can be registered in parallel. The experiments are conducted in the incubator. To ensure a temperature of 37 °C for the cell chip the incubator was adjusted to 34.5 °C to compensate for the additional heat production by the pre-amplifier box (see Fig. 2). The neuronal signals are amplified and filtered before online visualization of their patterns by a special PC (Plexon Inc., Dallas, TX, USA). Fig. 3 gives a schematic representation of the experimental procedures and the setup.

5. Results and discussion

5.1. Behavior of the wave-guide

The wave-guide setup was tested for no considerable field decrease over the frequency range from 1.9 GHz to 2.2 GHz in the propagating wave mode. The control experiment was conducted with a cell-free chip carrying the nourishing trough with 200 µl DMEM.

Fig. 4 shows results of transmission and reflection measurements of the wave-guide with a chip carrying a trough filled with 200 µl DMEM. In both cases, with and without chip, the parameters were excellent in the range from 1.9 GHz to 2.2 GHz. The reflection without chip was below 20 dB and still below 18 dB in the presence of the chip. The corresponding losses in transmission were 0.1 dB and 0.2 dB, respectively.

5.2. Field distribution for the propagating and standing wave modes

The conductivity of the nourishing solution $\sigma = 1.8$ S/m (37 °C) was checked with a conductometer. The relative permittivity ε_r was extrapolated to about 70 [10]. The electric field intensity distribution in then measuring volume has been calculated for an incoming power of $P_{inc} = 1$ W using the software CST Microwave Studio™, Ver. 5.1. (CST GmbH, Darmstadt, Germany). Fig. 5 presents distributions in the sample

Table 1
Equations to describe the measured temperature patterns (see T_d in Fig. 8) within time intervals of different exposure power

Time interval i: t_{start}, t_{stop}	Line texture	Equation $T_i(t)$
0 min, 27.7 min		$T_1(t) = 31\ °C + 5.95\ °C\left(1-\exp\left(-\frac{t}{1.95\ \text{min}}\right)\right)$
27.7 min, 51.5 min		$T_{2a}(t) = 36.9\ °C + 1\ °C\left(1-\exp\left(-\frac{t-27.7\ \text{min}}{1.95\ \text{min}}\right)\right)$
27.7 min, 51.5 min		$T_{2b}(t) = T_{2a}(t) + 0.15\ °C\left(1-\exp\left(-\frac{t-27.7\ \text{min}}{27\ \text{min}}\right)\right)$
51.5 min, 91 min		$T_3(t) = 37.4\ °C + 0.6\ °C\exp\left(-\frac{t-51.5\ \text{min}}{2.24\ \text{min}}\right)$
91 min, 141 min		$T_4(t) = 37.2\ °C + 0.2\ °C\exp\left(-\frac{t-91\ \text{min}}{2.45\ \text{min}}\right) -0.0026\frac{°C}{\text{min}}(t-91\ \text{min})$
141 min, 200 min		$T_5(t) = 37.1\ °C - 0.0047\frac{°C}{\text{min}}(t-141\ \text{min})$

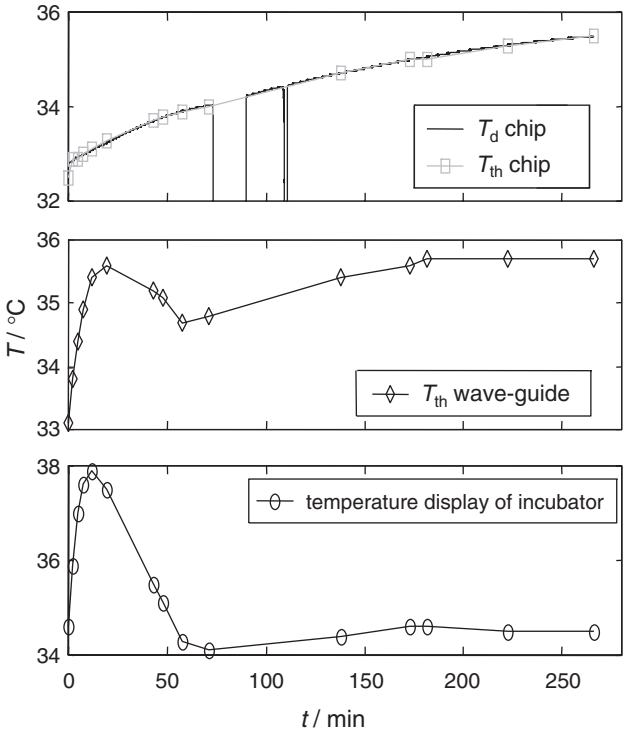

Fig. 10. Temperature patterns without applied EMF. A chip with 200 µl DMEM was installed in the wave-guide. Top: temperature measured by the temperature diode (T_d chip) on the chip (lined) and by a temperature sensor (T_{th} chip) in the vicinity of the chip (boxes). Diode malfunction appeared two times. Center: temperature measured at the outer rim of the wave-guide by a second temperature sensor (T_{th} wave-guide). Bottom: incubator temperature.

volume for the propagating and the standing wave modes. The modes differ in the homogeneity of the field distribution over the active chip area.

For the propagating wave, a field strength gradient was obtained over the chip. In the standing wave mode, the constructive interference leads to a largely homogeneous field in the chip trough.

5.3. Signal recording

Active chips were mounted to the wave-guide and connected to the special PC (Plexon Inc.) via a homemade pre-amplifier box. Fig. 6 shows the chip with neuronal and glial cells. Before an actual experiment was started, the signals of all electrodes were checked for neuronal activity. After 1 h, the incoming signals were usually stable and the active channels could be selected. The action potentials from these channels were graphically separated from disturbing noise using the MEA Server program (Plexon Inc.) before starting the record for the actual experiment. Measurements were conducted for up to 14 h. The NeuroExplorer software (Plexon Inc.) allowed for a statistical analysis of the differences between periods with and without EMF exposure. For the chip presented in Fig. 7, action potentials were registered from 31 of the 58 channels of the microelectrode array. Examples are given in Fig. 8 (8 channels over the whole experimental time of about 14 h).

Fig. 8 shows an example for the different behavior of the neuronal signals. For experiments, we used chips some hours before their feeding time. These chips showed the highest electric activity. Feeding prior to the experiments dramatically lowered the activity and was therefore avoided. Nevertheless, neuronal activity decreased after about 5 h, suggesting no longer periods of permanent registration. The probable reason was metabolic stress, resulting in a lower spike rate (Fig. 8). The consumptive use of the chips was also reflected in the color of the nourishing solution containing the pH indicator phenol red. At the end of the experimental time, the solution turned yellowish reflecting the acidification of the solution. Therefore, experiments were not extended more than 5 h.

5.4. Temperature course during CW EMF exposure

The application of CW fields of varying power led to characteristic temperature patterns (Fig. 9). These patterns were registered by the on-chip temperature diode (T_d) and a temperature sensor located outside the wave-guide in close vicinity to the chip (T_{th}). Accordingly, the temperature reflected by T_d is very similar to that experienced by the neuronal network. To reduce the number of electronic heat sources inside the incubator, the terminating resistor of the wave-guide was located outside the incubator. Nevertheless, we found a complex interplay of the temperature regulation of the incubator, the heat production of the pre-amplifier box and the applied EMF power as registered by T_d. The air exchange in the incubator during the chip installation initiated a smooth, long regulating process over about 200 min as registered by T_{th}. The same process is reflected by T_d that even dropped below 37 °C between 170 and 220 min. Analytic functions, describing the course of T_d, are given in Table 1 and plotted in Fig. 9 (center).

Crucial parameters of these functions are the maximal temperature differences in front of the exponential terms as well as the time constants given in the exponents. We assume that the faster processes (time constants around 2 min) arise from the temperature adaptation responses of the electronic devices. These may either result from passive or active processes, as the mounting of chips at room temperature or the EMF-induced heat dissipation. The slower processes were fitted by an exponential function with a time constant of around 30 min or even by linear terms (see Fig. 9, from 91 to 200 min). The first temperature increase in Fig. 9 reflects the adaptation of the chip to 37 °C, i.e., its thermal equilibrium without EMF application. The equilibrium is determined by the incubator temperature of 34.5 °C and the heat input from the pre-amplifier box. The second interval (27.7–51.5 min) reflects two contributions, the temperature increase induced by the EMF power absorption and the slow continuing temperature regulation process of the incubator (compare T_{th} and T_d curves). One should keep in mind that the firing rate may be very sensitive to temperature changes. For example, warm-sensitive neurons possess a firing rate increasing with 1.07 Hz±0.06 Hz per degree [11]. We suppose that a temperature increase of approximately 1 °C is

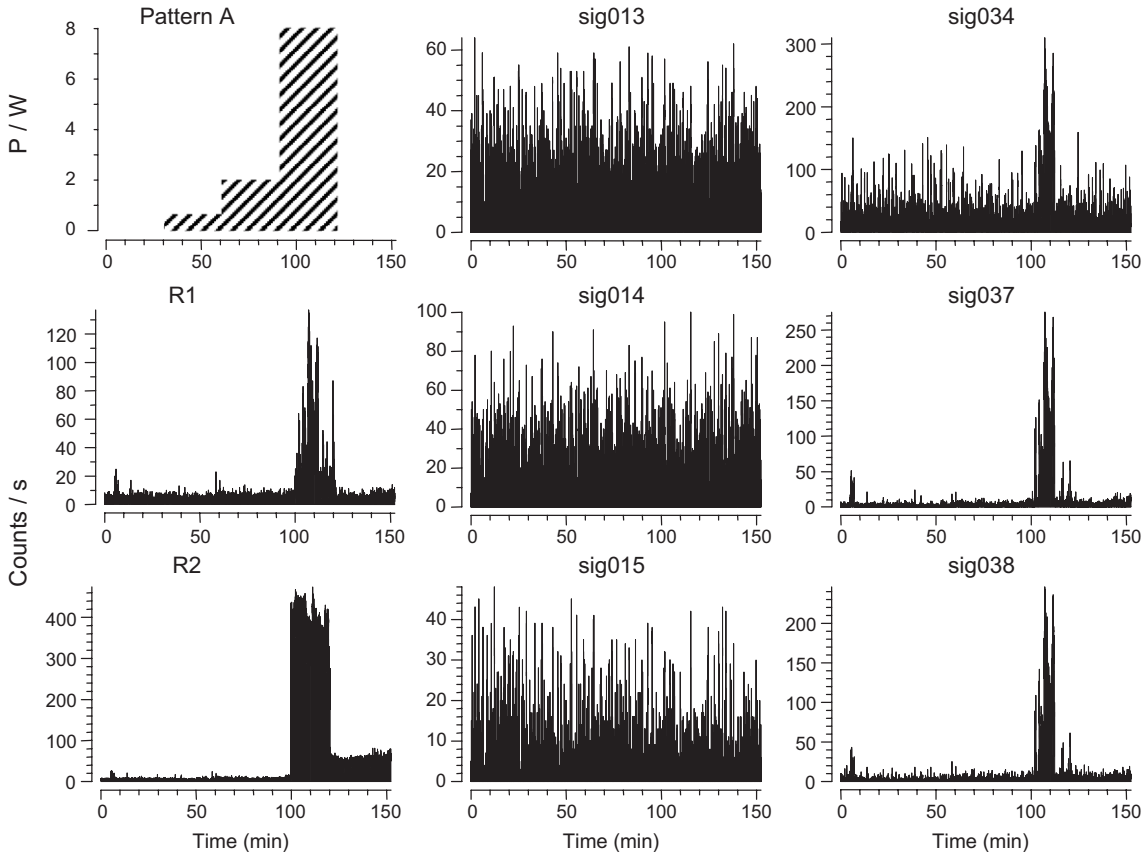

Fig. 11. Three classes of signals recorded from the same chip that was exposed according to the pattern given in the upper left corner. Reference electrodes (R1, R2) were chosen to not exhibit any neuronal activity. Nevertheless, these electrodes may pick up a noise signal when exposed to higher power levels. The second and third columns show signals from selected electrodes with neuronal activity.

also critical for the physiological status of the neuronal networks and should not be exceeded (compare to fever). In our experiments, this 1 °C threshold is reached at an EMF power input of approximately 8 W. In principle, the EMF power absorption by the nourishing solution can be compensated by an appropriate reduction in the temperature adjusted at the incubator for every power level. Nonetheless, dynamically this is not possible for our current setup, since similar time constants for the heating and regulating processes would be required. The time constant of the incubator was determined in a very simple way (Fig. 10). A temperature regulation process was enforced by the air exchange due to the opening of the incubator (cooling). 0 min corresponds to the first measuring point. Obviously, the incubator regulator overcompensates the induced temperature drop within approximately 15 min (first regulating process). After this process, the steady warming of the waveguide and the chip follows. Furthermore, this heat continues to warm the DMEM in the nourishing trough until the end of the experiment (70–180 min, second regulating process). For future experiments, we will establish a resistor heating with a short time constant directly attached to the chip to optimize the temperature regulation. An alternative approach would be to compare the neuronal activity of a certain chip adjusted to the same temperature, either by the incubator alone or in combination with EMF-induced heating. For this, the temperature effect of EMF absorption by the nourishing fluid for various fluid volumes must be determined.

5.5. Signal acquisition under EMF exposure

The EMF exposure patterns are given as inserts in Figs. 11 and 12 and Table 2.

A comparison of the neuronal signals within the different experiments show similar firing rates of 50–400 counts/min in all experiments, i.e., under EMF exposure according to the patterns A (Fig. 11) or B (Fig. 12) as well as in the long-term experiment (Fig. 8). Different types of electrode signals could be identified with and without EMF exposure. Most of the electrode signals were noisy, no matter whether the chips were cell free or covered by a glia cell layer. For some electrodes EMF application induced a strong increase in the noise level that was, surprisingly, not mandatory related to the field on-period (Fig. 12 corresponding to exposure pattern B, Fig. 13 corresponding to cell-free chip test exposure). Clear neuronal signals were detected from two classes of electrodes. In the first class, EMF application induced a strong increase in the noise amplitude (Figs. 11 and 12, sig034, sig037, sig038), whereas in the second class, no significant increase was detected (Figs. 11 and 12, sig013, sig014, sig015).

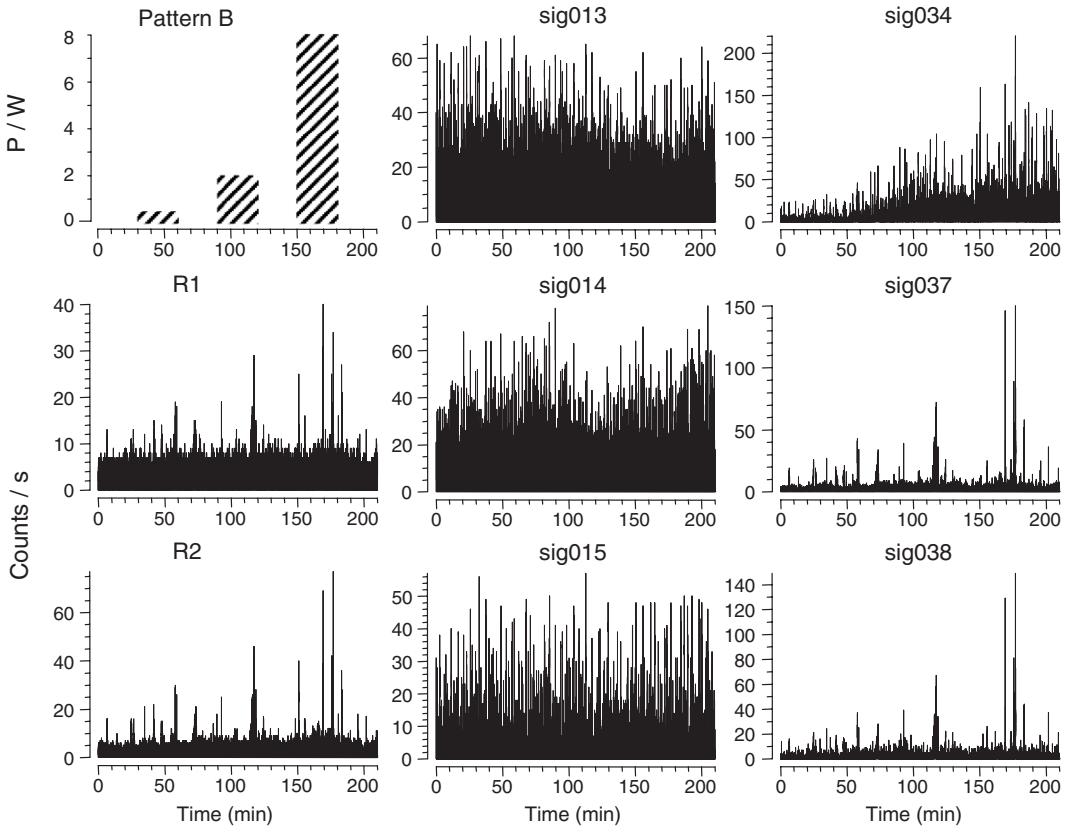

Fig. 12. Three classes of signals recorded from a chip exposed to the pattern given in the upper left corner. For further explanations, see caption of Fig. 11.

5.5.1. Pattern A

An on-chip temperature increase was found for increasing EMF power (Fig. 9). In the same test (Pattern A, Fig. 11), the reference electrodes (R1 and R2) were affected by the EMF above a certain power level. Since R1 and R2 were covered by glia, the signals differed from the signals of cell-free chips exposed to EMF (Fig. 13). One can speculate that the presence of glia alters the effective electrodes impedance. For electrodes with neuronal signals and EMF-induced noise, the electric signature of the neuronal networks were superimposed with distinct disturbing signals (Figs. 11 and 12, sig034, sig037, sig038). This was only observed during the exposure to 8 W EMF power (within 90 and 120 min). However, the disturbing signals appeared only after 100 min and disappeared at field-off (please note the contrast to pattern B). Therefore, a direct electronic pick-up of the emission can be excluded. One can hypothesize that a continuously increasing temperature and/or related electrochemical electrode-interfacial processes are responsible for the effect. On the other hand, after field-off the signal intensities at the reference electrodes immediately decreased to the normal noise level. We tested that the field application did not cause any irreversible damage to the pre-amplifier input stage. Nevertheless, even though the pre-amplifier possesses a high-frequency cut-off of about 10 kHz we cannot fully exclude interferences in the electronic signal processing.

Table 2
Two different EMF power patterns were applied to the micro-sensor chips

Pattern	0.5 h	1 h	1.5 h	2 h	2.5 h	3 h	3.5 h
A	Off	0.5 W	2 W	8 W	Off		
B	Off	0.5 W	Off	2 W	Off	8 W	Off

In both patterns, the maximum power input of 8 W was applied for 30 min. Pattern A: stepwise increase. Pattern B: stepwise increase with off periods.

5.5.2. Pattern B

EMF application according to pattern B resulted in fewer disturbing signals (Fig. 12). This suggests a time-dependent process to be involved resulting in a positive effect of a longer chip cooling period during field-off. Therefore, we prefer pattern B over A.

6. Outlook

In the future, post-processing will allow us to discriminate against noise using a data analysis tool (Offline Sorter, Plexon Inc.). Fig. 14 demonstrates the power of the tool for the separation of the neuronal signal from EMF-induced noise. Nevertheless, it will be important to exclude high-noise signals from the neuronal recordings.

Our preliminary results on the neuronal network activity demonstrate the high potential of our approach. Our wave-guide setup allows for a CW EMF exposure in the frequency range from 1.9 GHz to 2.2 GHz in the propagating and standing wave modes. In the future also, a generic UMTS signal will be applied in the propagating wave mode. The temperature compensation

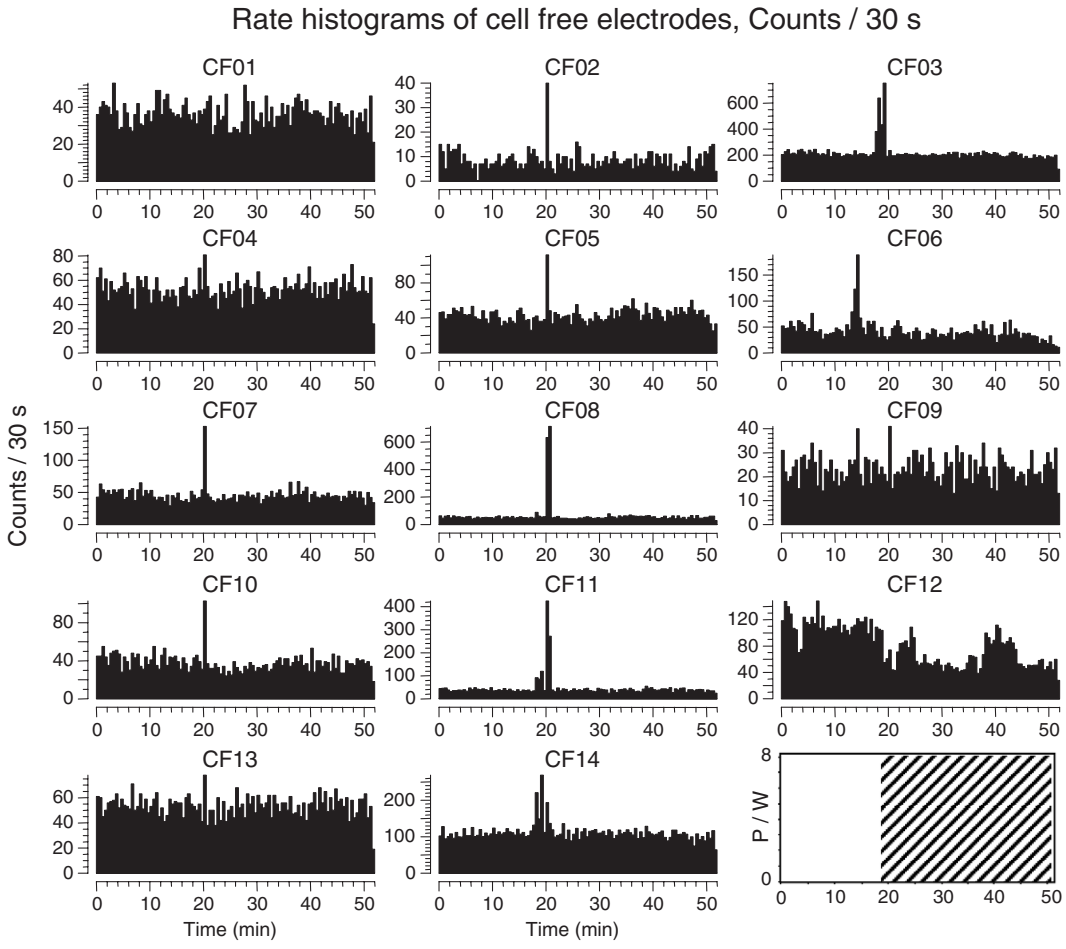

Fig. 13. Signal recordings over time. Chip without cells; trough filled with deionized water. The EMF was applied after 18 min.

can be improved. Despite the electric activity of the network, also, others, such as metabolic parameters, can be observed. Finite-element methods, as applied in the field calculations, will also allow for the calculation of the specific absorption rate (SAR) in the nourishing solution. In summary, no basic statements on possible EMF effects on neuronal networks can be made at the current state of our research.

Acknowledgements

This study has been supported by Grant StSch 2002 0418A from the Bundesamt für Strahlenschutz (Federal Office for Radiation Protection). The authors thank Dr. S. Homma for helpful discussions and the staff of the IZT (Institute for Cell Technology, Rostock-Warnemuende, Germany) for cooperation. The staff of the core facility "animal house" of the Department of Surgery at the University of Rostock's Medical Faculty is acknowledged for the reliable supply of mice. We are grateful to Prof. R. Meyer, Univ. of Bonn, for the kind provision of a wave-guide for preliminary tests. We thank Dr. G. Friedrich from Forschungsgemeinschaft Funk for the donation of a generic UMTS-signal generator that was developed in the group of Prof. V. Hansen, Univ. of Wuppertal. We thank Mr. R. Sleigh for his help with the language.

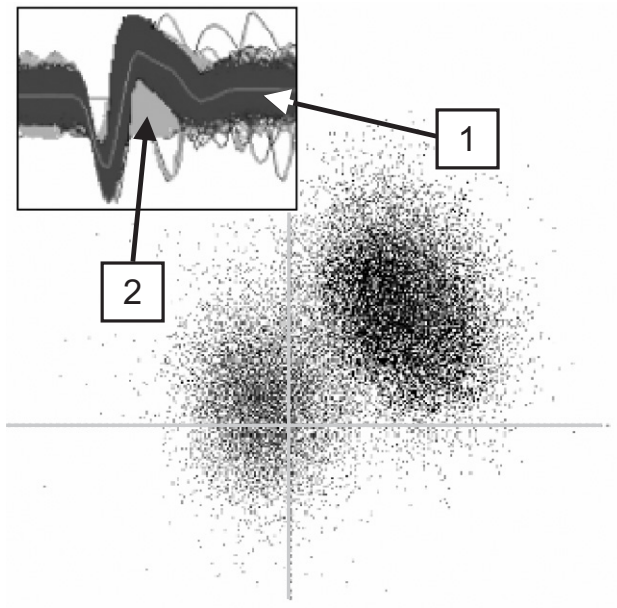

Fig. 14. Extraction of neuronal signals (1) from a high-noise (2) input. The Offline Sorter program (Plexon Inc.) generates two clusters in a 2D plot. Left corner: neuronal signals in waveform ($n=500$). Middle: the neuronal signal (dark grey) is significantly separated from the noise (grey).

References

[1] W.H. Baumann, E. Schreiber, G. Krause, A. Podssun, S. Homma, R. Schrott, R. Ehret, I. Freund, M. Lehmann, Cell monitoring system with multiparametric CMOS micro-sensor chips, Proceedings μ-TAS, vol. 2, 2004, pp. 554–556.

[2] R. Garrido, Marks of P. Mattson, B. Hennig, M. Toborek, Nicotine protects against arachidonic-acid-induced caspase activation, cytochrome *c* release and apoptosis of cultured spinal cord neurons, J. Neurochem. 76 (2001) 1395–1403.

[3] G.W. Gross, Simultaneous single unit recording *in vitro* with a photoetched laser deinsulated gold multimicroelectrode surface, IEEE Trans. Biomed. Eng. 26 (5) (1979) 273–279.

[4] G.W. Gross, A.N. Williams, J.H. Lucas, Recording of spontaneous activity with photoetched microelectrode surfaces from mouse spinal neurons in culture, J. Neurosci. Methods 5 (1–2) (1982) 13–22.

[5] V. Hansen, J. Streckert, Feldtheoretische Simulation der Hohlleitungs-Experimente zum Einfluß hochfrequenter elektromagnetischer Felder auf humane periphere Lymphozyten, FGF, Ed. Wiss. 14 (1998) 14–23.

[6] M. Lehmann, W. Baumann, M. Brischwein, H.J. Gahle, I. Freund, R. Ehret, S. Drechsler, H. Palzer, M. Kleintges, U. Sieben, B. Wolf, Simultaneous measurement of cellular respiration and acidification with a single CMOS ISFET, Biosens. Bioelectron. 16 (2001) 195–203.

[7] H. Meinke, W. Gundlach, in: K. Lange, K.-H. Löcherer (Eds.), Taschenbuch der Hochfrequenztechnik, Sringer-Verlag, Berlin, 1992.

[8] W.J. Parak, M. George, M. Kudera, H.E. Graub, J.C. Behrends, Effects of semiconductor substrate and glia-free culture on the development of voltage-dependent currents in rat striatal neurones, Eur. Biophys. J. 29 (2001) 607–620.

[9] H. Ndoumbè Mbonjo Mbonjo, J. Streckert, A. Bitz, V. Hansen, A. Glasmachers, S. Gencol, D. Rozic, Generic UMTS test signal for RF bioelectromagnetic studies, Bioelectromagnetics 25 (2004) 415–425.

[10] J. Sudsiri, D. Wachner, J. Gimsa, On the temperature dependence of the dielectric membrane properties of human red blood cells, Bioelectrochemistry 70 (2007) 134–140 (this issue). doi:10.1016/j.bioelechem.2006.03.010.

[11] J.D. Griffin, J.A. Boulant, Temperature effects on membrane potential and input resistance in rat hypothalamic neurones, J. Physiol. 488 (1995) 407–418.